

A Strategy for High-Resolution Ensemble Prediction

Part I: Definition of Representative Members and Global-Model Experiments

F Molteni¹, R Buizza, C Marsigli², A Montani², F Nerozzi² and T Paccagnella²

Research Department

¹ Current affiliation: CINECA, Centro di Calcolo Inter-Universitario,
Casalecchio di Reno (Bo), Italy

² ARPA-Servizio Meteorologico Regionale Emilia Romagna, Bologna, Italy.

May 2001
Also Q. J. R. Meteorol. Soc., 2001, in press



ABSTRACT

In the last few years, tens of alternative weather forecasts have been made available to forecasters by operational ensemble prediction systems. In many forecasting applications, it is useful to identify (possibly in an objective way) a few representative ensemble members, deemed to represent the most interesting weather scenarios. In this paper, a strategy to select representative members (RMs hereafter) from an ensemble prediction is developed, and applied to four cases of medium-range ensemble forecasts performed with the ECMWF Ensemble Prediction System (EPS). The four case studies correspond to events of very intense rainfall (leading to localized floods) in the alpine region, selected as benchmarks for numerical simulations in the Mesoscale Alpine Project. The RM selection procedure uses a cluster analysis of the ensemble forecasts as its first step. For each cluster, a RM is defined to be the member with the smallest ratio between its average distance from the members of its own cluster and its average distance from the members of the other clusters. Distances are computed either using a l^2 -norm applied to 700 hPa geopotential height fields or a l^1 -norm to precipitation fields.

RMs are compared with cluster centroids in the four case studies of extreme rainfall. By definition, RMs are characterized by a synoptic-scale atmospheric flow similar to the flow of the corresponding cluster centroid, but they contain more small scale features, especially in the prediction of weather parameters such as precipitation.

RM initial conditions can be used to initiate higher-resolution global forecasts; alternatively, RMs may be used to define initial and boundary conditions for nested high-resolution forecasts with limited-area models. Integrations of RMs with the ECMWF global model at T₃₁₉ horizontal resolution (compared to the T₁₅₉ resolution used in the EPS) were performed. Results indicate that each higher-resolution forecast, started from a RM initial conditions, remains closer to the low-resolution RM than to other ensemble members, but it provides a more detailed forecast of weather parameters, especially in regions of complex topography. Experiments with a nested limited-area model, started from the same set of RMs, are described in a companion paper (*Marsigli et al. 2000*)

1. INTRODUCTION

Probability forecasts of weather events are daily produced by global ensemble systems at the National Center for Environmental Prediction (NCEP, *Toth & Kalnay 1993*), at the European Centre for Medium-Range Weather Forecasts (ECMWF, *Molteni et al. 1996*) and at the Recherche en Prévision Numérique (RPN, *Houtekamer et al. 1996*). Ensemble systems allow estimating in an objective way the probability of different weather patterns or regimes. Moreover, the combined use of probabilistic and deterministic forecasts, given for example by the control or the ensemble mean, has made possible to gauge the predictive skill of the deterministic forecast itself.

The three operational ensemble systems developed at NCEP, ECMWF and RPN cover the whole globe, and they have been constructed to provide the most useful information on the medium range (say after forecast day 2-3) and on synoptic scales (with a resolution of 100-200 km). The ECMWF Ensemble Prediction System (hereafter EPS), which is the operational global ensemble with the highest resolution at the time of writing, has been tuned for predictions in the medium-range, say from forecast day 2 to day 10. The experiments described in this work are based on an EPS configuration with 50 perturbed and 1 unperturbed

(i.e. starting from the ECMWF analysis) members at T₁159L31 resolution, equivalent grid point resolution of about 120 km at mid latitudes (*Buizza et al.* 1998). (At the time of writing, the EPS runs with an increased vertical resolution of 40 levels.)

Computer resources availability is the main cause of the current limitation imposed on the horizontal resolution of ensemble systems. At ECMWF, for example, the EPS has been tested at horizontal spectral triangular truncation T₁319, but the cost of running 51 non-linear integrations at this resolution is too high to make it operationally feasible with the current computer resources.

One of the problems of the current 51-member T₁159 EPS is the poor forecast skill in predicting high rainfall amounts (more than 10mm/12h), especially during the warm season when predictability is limited to 3 days over Europe (*Buizza et al.* 1999a). The quality of the probabilistic forecasts could be improved by integrations at higher resolution, characterized by a better model representation of orographically related processes, which have a strong influence for example on precipitation prediction over central Europe and the Mediterranean region.

To overcome similar limitations of their global ensemble, NCEP developed the Short-Range Ensemble Forecasting (SREF) system to generate ensemble forecasts optimized for the 0-to-3-day range (*Tracton et al.* 1998). The NCEP SREF system, which has been running in experimental mode since 1995 (*Brooks et al.* 1995, *Hamill & Colucci* 1997), is composed of 25 members, run with a 80 km resolution versions of the NCEP's Eta and Regional Spectral Model, with initial conditions perturbed using global and regional bred vectors (*Toth & Kalnay* 1993) or defined using different in-house analyses. Results suggest, for example, that the SREF can be particularly useful when used for quantitative precipitation predictions (*Tracton et al.* 1998).

Another approach to short-range limited area ensemble which should be mentioned is the one followed by *Stensrud et al.* (1999), who created ensembles either by using different model physical parameterization schemes starting from identical (unperturbed) initial conditions, or by using the same model but starting from different randomly generated (*Errico & Baumhefner* 1987; *Du et al.* 1997) initial conditions. Their results suggest that varying the model physics is a reasonable and potentially powerful method to create an ensemble, especially in cases when the large-scale forcing for upward motion is weak.

A strategy of nesting a limited area model in a version of the ECMWF EPS targeted for Europe is under investigation by a joint research group including the Royal Netherlands Meteorological Institute (*Hersbach et al.*, 1999), Oslo University (*Frogner & Iversen*, 1999), the Regional Meteorological Service of Emilia Romagna, Italy (*S. Tibaldi & T. Paccagnella*, 1998, personal communication), and ECMWF. The first step of the strategy involves integrating a version of the EPS up to forecast day 5 with 50 T₁159L31 members, but with initial perturbations targeted to maximize the perturbation growth over Europe in the short range (2-3 days). Preliminary results from *Hersbach et al.* (1999) indicate that targeting the perturbations can improve probability predictions of rare events. Subsequent nesting of limited area models in this targeted EPS (or in the global ECMWF EPS) could provide probabilistic products at higher resolution.



This paper and a companion paper by *Marsigli et al.* (2000) describe the results of experimentation aimed at the development of a high-resolution ensemble system particularly suited for the prediction of extreme events. These events are often associated with the development of sub-synoptic systems, which reach their maximum intensity on relatively small regions and are strongly affected by the local topography. In these cases, a high horizontal resolution is essential to capture the intensity of the weather events. Therefore, to supplement the information provided by a global, synoptic-scale ensemble, it may be preferable to use the additional computer resources to run very few perturbed integrations at very high resolution, rather than adding a larger number of integrations with only a modest resolution increase.

To follow this strategy, one has to address the problem of the choice of a few alternative scenarios (among those represented by the individual members of the global ensemble) which one wants to explore in detail with the high-resolution runs. More specifically, given the 51 members of a T₁₅₉ EPS (or maybe, in the future, of a targeted EPS), one needs to define a few representative members (hereafter RMs) which identify relevant forecast states for the situation under examination. Once the RMs have been identified, high-resolution forecasts may be produced by running the ECMWF global model at T₃₁₉ resolution starting from the perturbed initial conditions associated with the RMs. Alternatively, the RMs can be used to define the initial and boundary conditions for nested high resolution limited area models. This strategy is based on the hypothesis that forecast errors up to forecast day 5 are dominated by initial condition rather than modeling uncertainties (*Richardson* 1998, *Harrison et al.* 1999), and therefore does not consider essential, at least in first place, to include the simulation of model errors. Despite this choice, the relative importance of the simulation of model uncertainties in limited-area high-resolution ensemble forecasting of precipitation is recognized, and the problem of the simulation of model errors will be addressed in the future, especially if this methodology leads to an operational implementation of a limited-area ensemble system.

CASE	EXTR EVENT DATE	ICS DATE
Vaison, 1992	22-23 September 1992	18 September 1992
Brig, 1993	23-24 September 1993	19 September 1993
Piemonte, 1994	5-6 November 1994	1 November 1994
Friuli-Venezia-Giulia, 1995	18-19 September 1995	14 September 1995

Table 1 Date of the extreme events and of the initial conditions from which ensemble integrations were performed. For all events, precipitation was accumulated between 12 GMT of the two dates of column 2, and the starting time of each integration was 12 GMT.

After this introduction, section 2 describes the methodology used to select the representative members. Results for the four case studies, based on the EPS on its current operational configuration, are reported in section 3. The relevance of the representative members and the application of the RM ensemble strategy

using the high-resolution ECMWF global model are discussed in section 4. Conclusions are drawn in section 5.

2. METHODOLOGY

2.1 The global ECMWF EPS

The EPS configuration used in this work can be schematically described as follows. Each ensemble member e_j can be seen as the time integration of the model equations

$$\frac{\partial e_j}{\partial t} = F(e_j; t) \quad (1)$$

starting from perturbed initial conditions

$$e_j(t=0) = e_0(t=0) + \delta e_j(t=0) \quad (2)$$

where $e_0(t=0)$ is the operational analysis at $t=0$ (*Molteni et al.* 1996, *Buizza et al.* 1998). The initial perturbations $\delta e_j(t=0)$ are generated using the T42L31 singular vectors of the linear version of the ECMWF model, computed to maximize the total energy norm over a 48-hour time interval (*Buizza & Palmer*, 1995), and scaled to have an amplitude comparable to analysis error estimates. The global ensemble experiments have been performed either at T₁159L31 or a T₁319L31 resolution, which are equivalent to a grid spacing of about 120 and 60-km resolution, respectively, at mid-latitudes. All forecasts have been run up to forecast time t+144h, but attention will be focused on the t+120h forecast range.

Note that all the experimentation reported in this work is based on the ECMWF EPS prior to the introduction of a stochastic simulation of random model errors due to physical parametrization (*Buizza et al.* 1999b).

2.2 The Representative Member (RM) sampling technique

Figure 1 is a schematic of the steps required to identify the RMs. First, starting from the day 5 forecast fields of geopotential height, a complete linkage cluster analysis (*Wilks* 1995) is performed to identify 5 clusters for a southern-European region (5°W-25°E; 35°N-53°N). By construction, cluster 1 always contains the control forecast. The choice of the space-time domain has been dictated by the interest in predicting extreme events in this area 5 days ahead. The number of clusters has been set to 5 because this is probably the maximum number of high-resolution integrations which can be performed to complement the EPS, either at ECMWF with a T₁319L31 version of the model, or at the Servizio Meterologico Regionale of Emilia Romagna (ARPA/SMR) with a limited-area model (see *Marsiglio et al* 2000).

The cluster analysis can be based on three circulation fields, wind vector v , wind direction v/v or vorticity ζ , derived from the geopotential height field. The geopotential height field at 700 hPa has been used instead of the more conventional 500hPa level because it gives a better representation of the influence of the Alpine orography on the lower troposphere flow. Since the southern-European area of interest is small compared to the large-scale features that affect any measure of similarity based on the geopotential field, functions of the derivatives of the geopotential (such as wind or vorticity) are preferred to the geopotential itself to identify



different circulation patterns. The comparison of the percentage of the ensemble variance explained by the 5 clusters (Table 2) indicates that higher percentages are achieved by choosing either the wind vector or the vorticity.

CLUSTERING VARIABLE	AVE % OF EXPL VAR	STD OF % OF EXPL VAR
Wind	54.8	4.5
Wind direction	45.2	3.9
Vorticity	55.7	9.9

Table 2 4-case average and standard deviation of the percentage of variance explained by 5 cluster for three different choices of the clustering circulation variable.

Once clusters have been constructed, RMs may be identified either using the circulation field f itself, or by considering a weather parameter of interest, in this case precipitation p . For each cluster C_l , the RM is defined as the EPS member with the smallest ratio between the average distance from the EPS members belonging to cluster C_l and the distance from the EPS members not-belonging to cluster C_l . Distances are computed using a l^2 -norm if the circulation field f is used to identify the RMs, or using a l^1 -norm if precipitation p is used.

More precisely, if the same circulation variable f is used both for clustering and for defining RMs, the RM of cluster C_l is defined as the i -th EPS member with the smallest *representativity index* $RI(f)_i$

$$RI(f)_i = \sqrt{\frac{\langle |f_i - f_j|^2 \rangle_{j \in C_l}}{\langle |f_i - f_j|^2 \rangle_{j \notin C_l}}} \quad (3)$$

If precipitation p is used the *representativity index* $RI(p)_i$ is defined as

$$RI(p)_i = \frac{\langle |p_i - p_j| \rangle_{j \in C_l}}{\langle |p_i - p_j| \rangle_{j \notin C_l}} \quad (4)$$

and RMs may also be defined by selecting the cluster member with the smallest value of this index. In Eqs. (3, 4) averages are computed considering all the ensemble members belonging (in the numerator) or not-belonging (in the denominator) to cluster C_l , inside the southern-European area and weighting each grid point by the cosine of the latitude.

Given a partition into clusters based on the circulation variable f , one can verify whether such partition is also meaningful for the precipitation field p by comparing the $RI(f)$ and $RI(p)$ indices for the same ensemble members. If there were no relationship between the distances computed using the f and p fields, the $RI(p)$ index would be much larger than $RI(f)$, and would be close to 1. Conversely, similar values of the two

indices are indicative that members of the same (circulation) cluster are also close to one another when distances are based on precipitation. We have verified that, for any of the three circulation variables used in the cluster analysis, the difference between $RI(f)$ and $RI(p)$ for the same ensemble member were generally comparable to the differences between $RI(f)$ indices of different members of the same cluster.

Since the values of $RI(p)$ are indicative of how well the circulation-based clustering “fits” the precipitation fields, one can use this criterion to choose which of the three circulation variables is most suitable to define weather scenarios where precipitation is a key element. The first three columns of Table 3 show the 4-case average $RI(p)$ for RMs identified by the same circulation variable used to define the clusters. Results indicate that wind vector v is the circulation variable that guarantees the lowest precipitation indices $RI(p)$. By contrast, the last column of Table 3 lists the 4-case average $RI(p)$ for RMs identified using precipitation. Again, clustering based on wind vector v provides the best results. Note that, by definition, the $RI(p)$ indices of precipitation-RMs are smaller than the $RI(p)$ indices of circulation-RMs. However, the relative small difference between the $RI(p)$ of the two set of RMs (especially for the wind-vector clustering) is another indication of the close relationship between circulation and rainfall patterns in these case studies.

CL VARIABLE	VARIABLE USED TO DEFINE THE RM			
	Wind	Wind direction	Vorticity	precipitation
Wind	0.65	---	---	0.62
Wind direction	---	0.71	---	0.66
Vorticity	---	---	0.69	0.65

Table 3 Average representativity index $RI(p)$ for the precipitation fields of circulation-RMs (column 1-3) and of precipitation-RMs, computed from cluster analyses using wind vector (row 1), wind direction (row 2) and vorticity (row 3) as circulation variable. See text for further explanation.

Once a particular circulation variable (and consequently a certain cluster partition) has been selected, one is left with the option of choosing one of the two possible definitions of RMs, either from the circulation or from the precipitation fields. This choice may depend on the particular forecasting application. For the case studies described in this paper, the emphasis is on the ability of the ensemble forecast to provide early warnings of intense rainfall events. On this basis, we have chosen to define the RMs using precipitation.

The fact that the cluster analysis is based on an upper-air variable, while the definition of RMs is based on a surface weather parameter, should not be seen as contradictory. As mentioned before, the purpose of the RM identification is to select a subset of ensemble members from which initial and boundary conditions are taken to run higher-resolution forecasts. These initial and boundary conditions are specified in terms of upper-air fields (initial values of surface parameters are not perturbed in the EPS). Therefore, when the application to nested limited-area modeling is considered, defining the clusters from the upper-air circulation is consistent with the fact that the information about the alternative weather scenarios is transmitted to the limited-area model through the upper-air circulation. On the other hand, when choosing which ensemble members are



most representative of these scenarios, one may wish to take surface weather parameters into account, especially in cases of extreme events.

Following these results, hereafter the wind vector field will be used as circulation variable, and the RMs will be identified using the precipitation field.

2.3 Performance assessment

Two variables are considered when assessing single deterministic or ensemble forecasts, the geopotential height field at 700 hPa and precipitation (the 700hPa level has been chosen instead of the more conventional 500hPa level because it gives a better description of the lower troposphere flow in the Alpine region). Consistently with Eqs. (3, 4), forecast errors are measured by the root-mean-square (rms) error of geopotential height and by the average absolute error of precipitation, with each grid point weighted with the cosine of the latitude. Probabilistic predictions of precipitation amounts are measured by the Brier score BS (*Brier 1950, Wilks 1995*),

$$BS = \frac{1}{n} \sum_{k=1}^n (y_k - o_k)^2 \quad (5)$$

where the index k denotes a numbering of the forecast/observed pairs, y_k is the forecast probability and o_k is 1 if the event occurs and 0 if the event does not occur. The BS is a measure of the distance between the predicted and observed probability distribution. The Brier score is negative oriented, with perfect forecasts scoring zero. Ensemble spread is measured as the average rms distance of the perturbed forecasts of geopotential height from either the control or the ensemble-mean. The ensemble-mean is defined as the mean among all 51 ensemble forecasts.

Geopotential height is verified against ECMWF analyzed fields. By contrast, precipitation is verified against an analyzed field constructed from observations available at the MAP (Meteorological Alpine Project) Data Center (web address: <http://www.map.ethz.ch/pubindex.htm>). The analyzed field of observed precipitation has been defined on a regular longitude/latitude grid with 1° degree spacing. Each grid-point value has been defined as a weighted average of all observations inside a 0.8° degree radius centred at the grid point, with weights depending on the distance between the grid point and the observation. Precipitation forecasts have been verified considering only the grid points of the Mediterranean region characterized by at least one observation available inside the 0.8° degree radius (generally speaking, these grid points cover about half of the Mediterranean region). Unless where stated, all verification measures have been computed inside the Mediterranean region.

3. CASE STUDIES

In this section, results from the clustering and RM selection performed on the T₁159 ensembles are presented for all case studies. Results of T₃19 integration started from the RM initial conditions are also shown, to assess to what extent global high-resolution runs can reproduce the weather scenarios identified from the lower-resolution ensembles.

All four case studies occurred during autumn (mid-September to early November), and are characterized by deep troughs or cut-off lows over Western Europe and the western Mediterranean. Sea surface temperatures over the Mediterranean are still relatively high in this season, which results in a high water vapor content of near-surface air masses in this region. This may often lead to very intense rainfall in regions where the large-scale ascent is reinforced by topographic forcing. A brief description of the synoptic situation during the individual cases is given below; the reader is referred to the companion paper *Marsigli et al.* (2000) for a more detailed description.

Table 4 lists the error of the control and the ensemble-mean forecasts (both for the 700 hPa geopotential height and precipitation), the ensemble spread (in terms of the 700 hPa geopotential height only) and the average precipitation amount. Two cases, Brig 1993 and Piemonte 1994, are characterized by large spread and large control (and ensemble-mean) rms errors for the 700 hPa geopotential height. These two cases are also characterized by the largest amounts of observed precipitation. Vaison 1992 is characterized by a relatively small spread and small control (and ensemble-mean) rms errors, and by the smallest amount of observed precipitation. In terms of precipitation, forecast errors tend to be proportional to the area-averaged observed value: for example, the control forecast for Brig 1993 has the largest absolute error, corresponding to the largest observed mean value, and the control forecast for Vaison 1992 has the smallest precipitation error. Piemonte 1994 is the case with the best (lowest) ratio between ensemble mean error and observed mean value of precipitation.

Hereafter, results for the four cases are discussed. Cluster centroids and RMs of the low-resolution T₁₅₉ ensembles are shown for all the cases, but for reason of space RMs of the high-resolution T₃₁₉ ensembles are shown for two cases only.

CASE	Z 700 ERROR (M)		Z 700 SPREAD (M)		PR ERROR (MM/D)		OB PR (MM/D)
	Control	Mean	Control	Mean	Control	Mean	
Vaison	14.9	11.5	15.4	9.0	7.6	6.9	7.0
Brig	27.0	37.3	50.9	45.9	19.2	17.8	17.1
Piemonte	37.4	31.8	40.9	34.4	17.7	12.7	15.0
Firuli	29.1	28.6	22.4	20.9	10.4	9.9	10.0

Table 4 700 hPa height: rms error of the control (column 2) and of the ensemble-mean (column 3), rms ensemble spread measured with respect to the control forecast (column 4) and rms ensemble spread measured with respect to the ensemble-mean (column 5). Precipitation: absolute mean error of the control (column 6) and of the ensemble mean (column 7), and average rainfall amount in the verification field (column 8). Values are computed for the southern-European region (5°W-25°E; 35°N-53°N).

3.1 Vaison-la-Romaine, France 1992

Extreme amounts of rain fell between 22 and 23 September 1992, when more than 200 mm/d of precipitation were observed in Provence, southern France, in the area of Vaison-la-Romaine (44°N; 5°E). At the time of the flooding, a large trough caused a southwesterly flow over the French coast, associated with intense convection activity (*Senesi et al.* 1996).



Figures 2 and 3 show, respectively, the clusters' centroids and the clusters' RMAs for the T₁159 ensembles (for each cluster, the centroid is the mean of all its members). Considering the 700 hPa atmospheric flow at 12GMT of 23 September (i.e. d+5 forecast), the centroids of the three most populated clusters (1, 2 and 3) are rather similar inside the south-European region (see Table 5 and Fig. 2), with a westerly/south-westerly flow over France, while the other two cluster centroids show a stronger cyclonic circulation. Centroid 2 (Fig. 2b) is the closest to verification, both in terms of 700 hPa geopotential height error and precipitation. Correspondingly, RM 2 (Fig. 3b) has the lowest 700 hPa geopotential height rms error and the lowest precipitation error. Note that RM 5 (Fig. 3e) predicts the highest amount of precipitation in the Vaison area. Overall, the differences between centroids are well captured by the corresponding RMAs.

Case	Cluster population				
	Cluster 1	Cluster 2	Cluster 3	Cluster 4	Cluster 5
Vaison	18	9	20	2	2
Brig	15	17	7	7	5
Piemonte	26	9	6	6	4
Firuli	16	3	18	3	11

Table 5 Clusters' population (by definition, cluster 1 contains the control forecast).

Figure 4 shows the T₁319 forecasts started from the RM initial conditions. Compared to the corresponding low resolution run, each high-resolution forecast (Fig. 4) has a similar synoptic scale circulation, but it includes more small-scale details especially in the precipitation field. Moreover, larger precipitation values are predicted by the high-resolution forecasts. At this resolution, RM 1 (Fig. 4a) has the lowest error for 700 hPa geopotential height, but RM 5 (Fig. 4e) has the lowest precipitation error and is able to predict quite correctly the location of the precipitation maximum over southern France. The comparison of Figs. 3 and 4 shows that each high-resolution forecast is more similar to the low-resolution forecast started from the same initial conditions than to the other T₁319 runs.

3.2 Brig, Switzerland 1993

Very heavy amount of precipitation fell between 23 and 24 September 1993 over Switzerland, with rain maxima greater than 100 mm/d recorded around Brig (44°N; 8°E). At the time of maximum precipitation, several mesoscale systems developed over the Alps, sustained by a meridional flow associated with a cut-off cyclone moving from the gulf of Valencia to the northeast of the Balearic Islands (*Benoit and Descagné 1995*).

This is the case with the largest ensemble spread and with the highest area-averaged amount of precipitation (Table 4). The very large ensemble spread influences the cluster populations, with each cluster including at least 5 elements (Table 5). Indeed, a large variability is shown in the atmospheric flow predicted by the cluster centroids (Fig. 5). The centroid of cluster 1 has by far the smallest error of 700-hPa height (Fig. 5a),

and also the smallest precipitation error, while the smoother flow pattern in centroid 2 is associated with the largest precipitation error (Fig. 5b).

The comparison of the cluster centroids (Fig. 5) and RMs (Fig. 6) confirms that each RM stays close to the centroid of its own cluster, while showing more detailed features. RM 1 (Fig. 6a) is by far the closest to the analysis, in terms of both synoptic circulation pattern and precipitation.

As for Vaison 1992, the synoptic scale flow predicted by each T₁319 RM integration (not shown) resembles closely the corresponding low-resolution prediction started from the same initial conditions. Comparing the low- and high-resolution RM 1, the low resolution RM has a slightly lower precipitation error; in this case, the high resolution forecast does not bring an improvement in the prediction of the rainfall field, at least in terms of objective scores.

3.3 Piemonte, Italy 1994

Heavy precipitation hit Piemonte (around 45°N; 8°E in north-western Italy) between 5 and 6 November 1994, with more than 250 mm/d observed. This event was related to a mid-tropospheric deep trough first localized over Spain and then slowly rotating anticlockwise, and to a southerly flow of warm and moist air at lower levels (*Buzzi & Tartaglione* 1995).

This is a case with a rather large spread, with a very large cluster number 1 including 26 ensemble members (see Table 5). The cluster centroids differ in the positioning of a deep trough over the Mediterranean region (Fig. 7), with the cluster-1 centroid (Fig. 7a) characterized by the smallest geopotential height error and the cluster-2 centroid (Fig. 7b) by the smallest precipitation error. Correspondingly, RM 1 and RM 2 (Figs. 8a,b) give the most accurate geopotential height and precipitation prediction, respectively.

As for the other two cases, each high-resolution forecast (Fig. 9) predicts an atmospheric flow similar to the corresponding low-resolution run (Figs. 8), but characterized by larger precipitation amounts. The high-resolution forecast with initial conditions defined by RM 1 (Fig. 9a) is the closest to verification, but RM 2 is almost as good; both forecasts show a very good prediction of the position of the precipitation maximum over the Piemonte and Liguria regions of north-western Italy. In this case study, the impact of high resolution is clearly beneficial, with a decrease in the precipitation error for the RMs of the two most populated clusters.

3.4 Friuli-Venezia Giulia, Italy 1995

Precipitation amounts up to 100 mm were observed in the first 12 hours of 19 September in the north-eastern Italian region of Friuli-Venezia Giulia (around 46°N; 12°E, at the north-eastern border of the Adriatic Sea). This region was affected by a south-westerly flow at 700 hPa, associated to a cut-off low centred over France, with warm and humid air masses moving from south and south-east towards the Friuli region (*Kerkman* 1996).



The cluster centroids (Fig. 10) differ mainly in their positioning and tilting of the cut-off low over southern Europe. The cluster 3 centroid (Fig. 10c) has the most accurate 700-hPa-height prediction, although with a weaker-than-observed cyclonic flow; on the other hand, the cluster-5 centroid (Fig. 10e) shows a deeper cyclone and the lowest precipitation error. The relationship between errors in the flow pattern and in precipitation is less clear in this case study than in previous ones: comparing the RMs, one finds that RM 2 (Fig. 11a) has the lowest 700-hPa height error but the largest precipitation error, while RM 5 (Fig. 11b) has a rather similar flow pattern to RM2, but shows the smallest precipitation error (the other RMs are not shown).

The discrepancy of geopotential height and precipitation scores is also reflected in the high-resolution RM forecasts, which as usual tend to predict more intense precipitation amounts. The higher resolution further improves the height score for RM 2 (Fig. 11c), but makes the precipitation score worse due to the larger (but somehow misplaced) rainfall amount; the precipitation error of RM 5 (Fig. 11d) is also much larger than its low-resolution counterpart. In this case however, because of the strong localization of the precipitation maximum in the Friuli region, the scores over the southern European area are not good indicators of the potential usefulness of the high-resolution forecast for flood-warning purposes. In fact, the lowest precipitation error is obtained with RM 3 (not shown), which tends to underestimate the rainfall amounts, while RM2 and RM5 show strong rainfall maxima close to the actual region of flooding.

3.5 Average results

The analysis of the four case studies has revealed a quite consistent relationship between cluster centroids, low-resolution RMs and their high-resolution counterparts. First of all, by comparing cluster centroids and RMs at the same resolution, a strong similarity is evident in the synoptic features of corresponding centroids and RMs. This confirms that the definition of the RMs given by Eqs. (3a,b) is appropriate.

A second (and less obvious) conclusion is that each high-resolution forecast remains closer to the low-resolution forecast started from the same initial conditions than to the other forecasts. This is confirmed, for the 700-hPa height field, by the comparison of the rms distance between forecasts started from identical initial conditions with the average ensemble spread, shown in Fig. 12. (In order to compute these statistics, and to perform the verifications described in the next section, a full 51-member ensemble has been run at T₁319 resolution for each case study). The average distance between corresponding low- and high-resolution forecasts (dotted curve) is definitely smaller than the average distance between control and perturbed forecasts at either low or high resolution (solid or dashed lines). If this were not the case, the high-resolution forecasts started from the RM initial conditions would have shown little relationship with the low-resolution RMs and centroids. As a further test of the relevance of the T₁159 clusters for the T₁319 ensembles, for each case the average values of the RI index (defined in Eq. (3)) was recomputed from the 700-hPa height fields of the T₁319 ensembles, using the cluster partition defined at low resolution. The average RI index, which is 0.66 for the T₁159 forecasts, shows only a modest increase (to 0.73) when T₁319 fields are used.

Finally, with regard to the usefulness of the high-resolution RMs for the prediction of the rainfall field, one may recall that in three out of four cases the smallest precipitation error among all RMs (at both resolutions)

has been achieved by a high-resolution forecast. It should be pointed out that apart for Brig 1993, in all the other cases the RM with the lowest precipitation error changes with resolution. This can be partly due to the fact that, using 5-cluster partitions in each case, the differences between some of the clusters may not be significant. A larger number of cases is needed to investigate whether this is the case.

4. RELEVANCE OF THE HIGH RESOLUTION RMS

A representation of the probability distribution of the precipitation field based on the 5 high-resolution RMs, with probability weights defined according to the cluster population, allows considerable savings of computational resources with respect to a full, 51-member T₃₁₉ ensemble. However, it is important to check whether such representation is *relevant*, that is if it captures the main features of the probability distribution for precipitation as defined by the whole 51 member ensemble.

The *relevance* of the 5 high-resolution RMs (and their corresponding probabilities) can be assessed by comparing the probability distribution for precipitation given by the following three ensemble configurations: E51H defined by a full 51-member T₃₁₉ ensemble, E5H defined by the 5 RMs with equal weight, and E5Hw defined by the 5 RMs but with a probability weight proportional to the cluster population.

Table 6 summarizes the average Brier score of configurations E51H, E5H and E5Hw for three rainfall thresholds (10, 30 and 50 mm/d). Configuration E51H has, on average, the lowest BSs for the 10 and the 30 mm/d thresholds, while configuration E5Hw has the lowest BS for the 50 mm/d threshold. Thus, despite the fact that the BS differences are small, results indicate that E5Hw performs slightly better than E5H. If one looks at each case separately (not shown), configuration E5Hw performs better than E5H in all cases for the 50mm/d threshold and it performs better than E5H 50% of the times for the 10 and 30mm/d thresholds. Further cases are needed to draw statistically significant conclusions on which of the two high-resolution configurations provides the best results. Nevertheless, results indicate that the 6-member high-resolution ensemble configurations based on only the 5 RMs plus the control can be a good substitute for the full 51-member high-resolution ensemble.

Configuration	Precipitation thresholds		
	10 mm/d	30 mm/d	50 mm/d
E5H	19.3	10.7	7.4
E5Hw	19.7	10.6	6.4
E51H	18.4	9.8	6.5

Table 6 Average Brier scores (multiplied by 100) for events of precipitation larger than 10, 30 and 50 mm/d, for the high-resolution configurations E5H (5 RMs only, no weight), E5Hw (5 RMs weighted by the cluster population, see text for details) and E51H (51 members). For each precipitation threshold, the lowest BS (which indicates the best forecasts) is highlighted in bold.

Figure 13 shows the ensemble-mean forecasts of configurations E51H and E5Hw, and reports the 700-hPa height rms error and precipitation mean-absolute error inside the southern European region at forecast day 5.



The two configuration produce very similar mean patterns of both geopotential height and precipitation. Comparing the ensemble-mean errors, the 51-member configuration has slightly better scores for 700-hPa height in 3 out of 4 cases, but the situation is reversed in favor of E5Hw when precipitation errors are compared (with a non-marginal improvement in the Piemonte case). If the unweighted E5H configuration were used instead of E5Hw, the RM ensemble would have a smaller precipitation error than the full ensemble only in one case (against three cases for E5Hw).

5. CONCLUSIONS

Operational ensemble forecasting systems implemented since 1992 (*Tracton & Kalnay 1993, Molteni et al. 1996, Houtekamer et al. 1996*) have changed the approach to numerical weather prediction, allowing the prediction of the probability density function of forecast states, and of its moments.

Ensemble systems cannot be run at the same resolution of single deterministic forecasts, because of limitations to computer resources. However, numerical experimentation with different ensemble configurations (e.g. *Buizza et al. 1998*) and operational experience in validating ensemble and deterministic forecasts has shown a beneficial impact of increased resolution for the prediction of surface weather parameters, especially in cases of extreme events and/or in region of complex topography.

In this work, a strategy has been developed to identify a few *representative ensemble members*, and to complement the ECMWF 51 member T₁59L31 ensemble system with a subset of perturbed high-resolution T₁319L31 forecasts, with initial conditions taken from the selected representative members. This approach would keep the computing requirements to an affordable level, but would still provide the users with high-resolution forecasts of alternative weather scenarios. Starting from a cluster analysis of the 51-member ensemble, representative members (RM) have been defined for each cluster as the element with the smallest ratio between the average distance from EPS members belonging to its own cluster and the average distance from members of the other clusters. Distances are computed using either a l²-norm applied to 700-hPa height fields or a l¹-norm for precipitation fields.

This study focused on four cases of intense precipitation events chosen from the case-study database of the Mesoscale Alpine Project. Computer resources availability limited the amount of experimentation, and the number of case studies had to be restricted to four.

Considering a southern-European region and focussing on 5-day forecasts, geopotential height and rainfall fields from the RMs have been compared with cluster centroids in the four case studies. Representative members are characterized by a synoptic-scale flow similar to their own cluster centroid, but they contain more detailed features, especially in the prediction of weather parameters such as precipitation. Thus, forecasters interested in assessing alternative weather scenarios may prefer to look at the RMs, rather than to the smoother cluster centroids, when comparing them with results from deterministic forecasts.

The initial conditions of T₁59 RMs have been used to initialize higher resolution T₁319 global forecasts. Results indicate that each T₁319 forecast remains closer to the “parent” low-resolution RM than to other ensemble members, but it provides a precipitation forecast with a more detailed representation of

topographic effect, and often with stronger rainfall maxima. In 3 out of 4 case studies, the high-resolution RM with the smallest precipitation error has a better score than any of the low-resolution RMs. Finally, a comparison of statistics from different ensemble configurations has shown that the probability distribution obtained from 5 high-resolution RMs (weighted according to the corresponding cluster population) provides a very good approximation to the distribution generated by a full 51-member T₁319 ensemble.

Despite the recognized need for a larger sample of case studies in order to draw statistically significant conclusions, this work shows that the representative member technique can be successfully applied to complement an operational ensemble prediction with a few selected high-resolution forecasts, in a way that aims to maximize the skill of the prediction at an affordable computational cost. A larger data-base is also needed to investigate the best methodology to combine the statistical information coming from the operational 51-member T₁519 ensemble with that derived from a few high-resolution forecasts started from the RM's initial conditions. Concerning the feasibility of an operational implementation of such a system, since running a T₁319 forecast cost approximately 8-times running a T₁519 forecast, the total cost of running 5 extra high-resolution forecast would be equivalent to running an extra 40 members at T₁519 resolution.

An aspect of limited-area ensemble prediction that was not addressed in this work is the relative impact of initial and boundary conditions. On this point, it is worth mentioning the results of *Du & Tracton* (1999), who indicated that ensemble spread is dominated by the influence of lateral boundary conditions after the first 2 forecast days.

A companion paper (*Marsigli et al.* 2000) reports on experiments in which initial and boundary conditions obtained from the EPS representative members are used in a high-resolution, limited-area ensemble system.



REFERENCES

- Benoit, R., & Desgagné, M., 1995: Application of the non hydrostatic MC2-LAM to the Brig 1993 flash flood event and the PYREX IOP3 foehn case. *MAP news letter* No3, October 1995, 24-26.
- Brooks, H. E., Tracton, M. S., Stensrud, D. J., DiMego, G. J., & Toth, Z., 1995: Short-range ensemble forecasting (SREF): report from a workshop. *Bull. Amer. Met. Soc.*, **76**, 1617-1624.
- Brier, G. W., 1950: Verification of forecasts expressed in terms of probabilities. *Mon. Wea. Rev.*, **78**, 1-3.
- Buizza, R., & Palmer, T. N., 1995: The singular-vector structure of the atmospheric general circulation. *J. Atmos. Sci.*, **52**, 1434-1456.
- _____, Petroliagis, T., Palmer, T. N., Barkmeijer, J., Hamrud, M., Hollingsworth, A., Simmons, A., & Wedi, N., 1998: Impact of model resolution and ensemble size on the performance of an ensemble prediction system. *Q. J. R. Meteorol. Soc.*, **124**, 1935-1960.
- _____, Hollingsworth, A., Lalaurette, F., & Ghelli, A., 1999a: Probabilistic predictions of precipitation using the ECMWF Ensemble Prediction System. *Weather and Forecasting*, **14**, 168-189.
- _____, Miller, M., & Palmer, T. N., 1999b: Stochastic representation of model uncertainties in the ECMWF Ensemble Prediction System. *Q. J. R. Meteorol. Soc.*, **125**, 2887-2908.
- Buzzi, A., & Tartaglione, N., 1995: Meteorological modelling aspects of the Piedmont 1994 flood. *MAP Newsletter*, **3**, 27-28.
- Du, J., Mullen, S., & Sanders, F., 1997: Short-range ensemble forecasting of quantitative precipitation. *Mon. Wea. Rev.*, **125**, 2427-2459.
- _____, & Tracton, S., 1999: Impact of lateral boundary conditions on regional model ensemble prediction. Research Activities in Atmospheric and Oceanic Modeling (edited by H. Ritchie), Report No. 28, CAS/JSC Working Group on Numerical Experimentation (WGNE), WMO/TD-No. 942, 6.7-6.8.
- Errico, R. M., & Baumhefner, D. P., 1987: Predictability experiments using a high-resolution and limited-area model. *Mon. Wea. Rev.*, **115**, 488-504.
- Frogner, I.-L., & Iversen, T., 1999: Targeted ensemble prediction for Northern Europe and parts of the North Atlantic Ocean. Report n. 107, Dept. of Geophysics, University of Oslo, P.O.Box 1022 Blindern, 0315 Oslo 3, Norway.
- Hamill, T. M., & Colucci, S. J., 1997: Verification of Eta-RMS short-range ensemble forecasts. *Mon. Wea. Rev.*, **125**, 2427-2459.
- Harrison, M. S. J., Palmer, T. N., Richardson, D. S., & Buizza, R., 1999: Analysis and model dependencies in medium-range ensembles: two transplant case studies. *Q. J. R. Meteorol. Soc.*, **125**, 2487-2515.
- Hersbach, H., Mureau, R., Opsteegh, J. D., & Barkmeijer, J., 1999: A short to early-medium range ensemble prediction system for the European area. KNMI pre-print 99-10, available from KNMI Library, Postbus 201, NL-3730 AE De Bilt, The Netherlands.201.

- Houtekamer, P., Derome, J., Ritchie, H., & Mitchell, H. L., 1996: A system simulation approach to ensemble prediction. *Mon. Wea. Rev.*, **124**, 1225-1242.
- Kerkmann, J. K. H., 1996: Case studies of severe convective storms in the Friuli area. *MAP Newsletter*, **4**.
- Marsigli, C., Montani, A., Nerozzi, F., Paccagnella, T., Tibaldi, S., Molteni, F., & Buizza, R., 2000: A strategy for high-resolution ensemble prediction. Part II: Limited-area experiments in four Alpine flood events. *Q. J. R. Meteorol. Soc.*, submitted.
- Molteni, F., Buizza, R., Palmer, T. N., & Petroliagis, T., 1996: The ECMWF ensemble prediction system: methodology and validation. *Q. J. R. Meteorol. Soc.*, **122**, 73-119.
- Richardson, D., 1998: The relative effect of model and analysis differences on ECMWF and UKMO operational forecasts. Proceedings of the ECMWF Workshop on *Predictability*, 20-22 October 1997, ECMWF, Shinfield Park, Reading RG2 9AX, UK.
- Senesi, S., Bougeault, P., Cheze, J. L., Cosentino, P., & Thepenier, R. M., 1996: The Vaison-la-Romaine Flash Flood: Meso-Scale Analysis and Predictability Issues. *Wea. & Forecasting*, **11**, 417-442.
- Stensrud, D. J., Bao, J.-W., & Warner, T. T., 1999: Using initial condition and model physics perturbations in short-range ensembles simulation of mesoscale convective systems. *Mon. Wea. Rev.*, submitted.
- Toth, Z., & Kalnay, E., 1993: Ensemble forecasting at NMC: the generation of perturbations. *Bull. Am. Meteorol. Soc.*, **74**, 2317-2330.
- Tracton, M. S., & Kalnay, E., 1993: Operational ensemble prediction at the National Meteorological Centre: Practical aspects. *Weather and Forecasting*, **8**, 379-398.
- _____, Du, J., Toth, Z., & Juang, H., 1998: Short-range ensemble forecasting (SREF) at NCEP/EMC. Proceedings of the *12th AMS/NWP Conference*, Phoenix AZ, 269-272.
- Wilks, D. S., 1995: *Statistical methods in the atmospheric sciences*. Academic Press, San Diego, California, 465 pp.

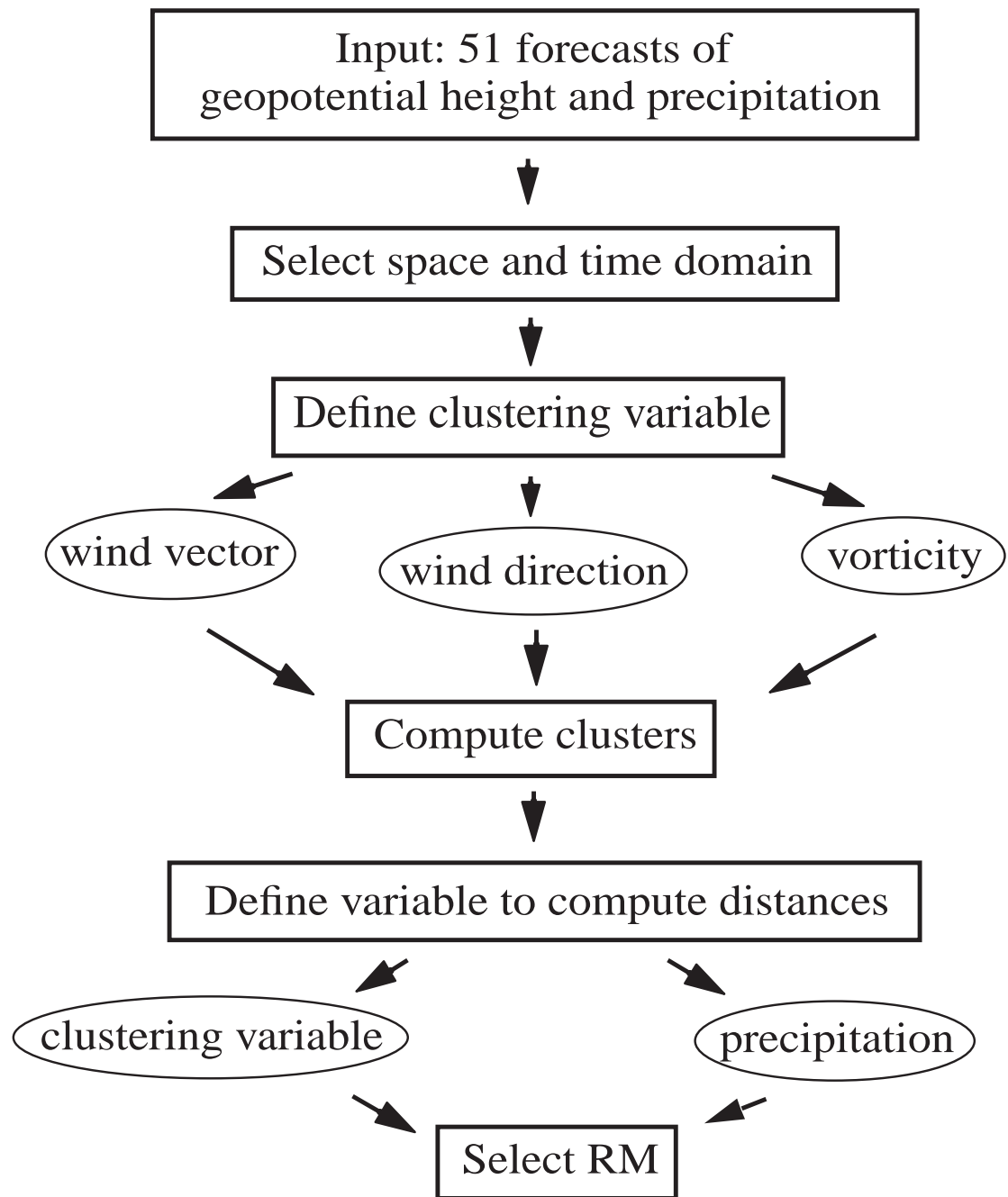


Figure 1 Schematic of the algorithm used to identify the representative members (RMs).

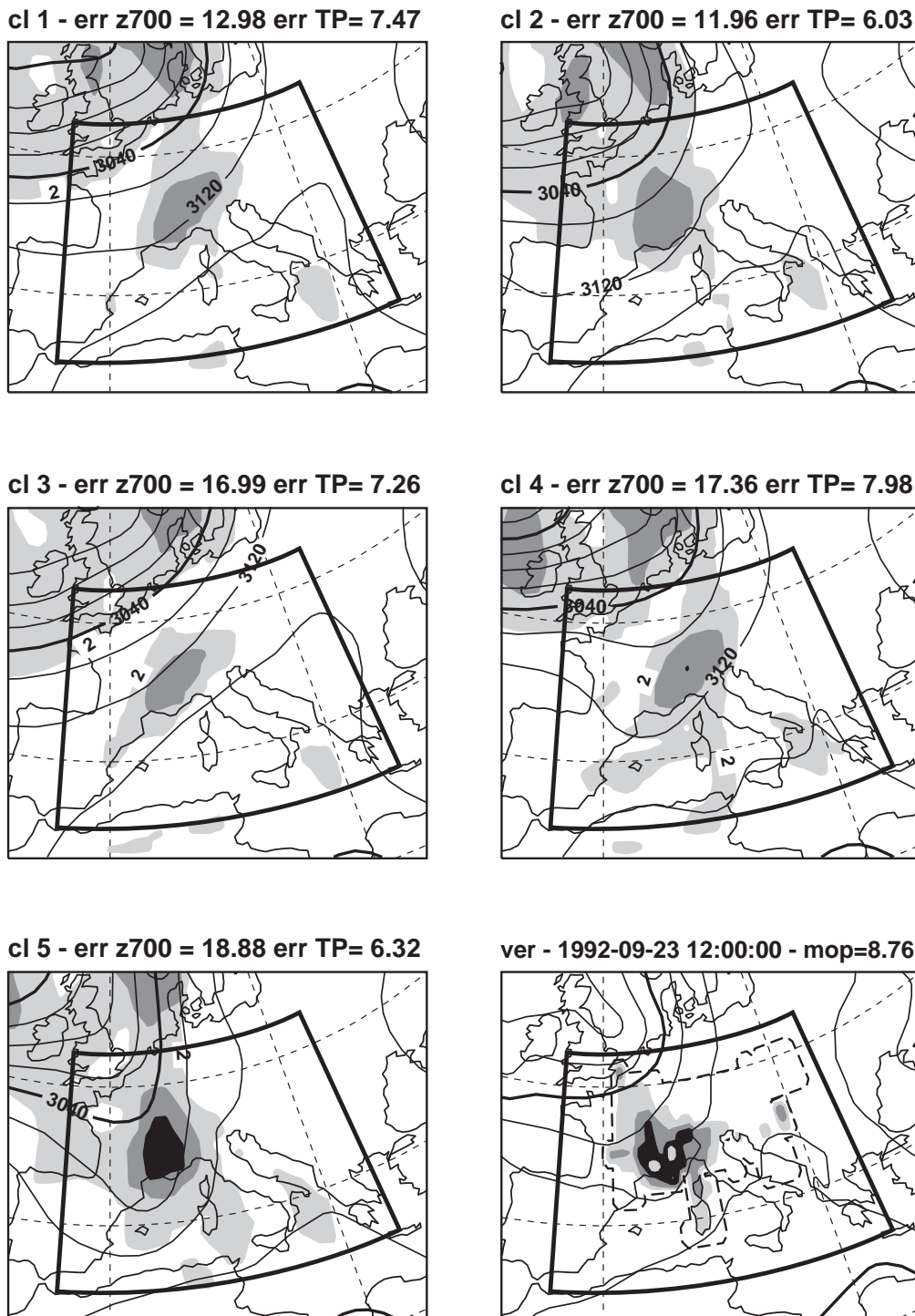
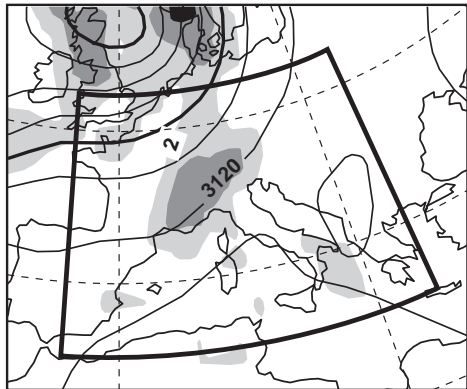
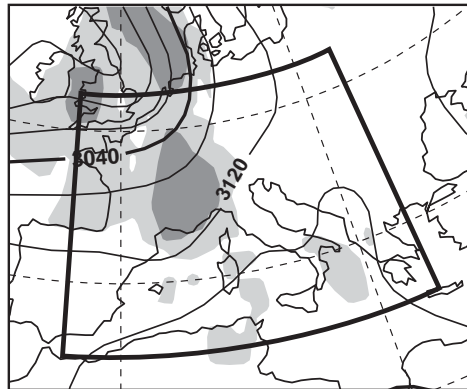


Figure 2 Vaison 1992. (a-e) cluster centroids of the 5-day EPS forecasts of 700 hPa geopotential height (valid at 12GMT of 23/9/1992) and of precipitation accumulated in the preceding 24-hours; (f) 700 hPa height analysis and observed precipitation. Height contour interval 40 m, and precipitation isolines 2, 10, 30 and 60 mm/d. In each panel, bold lines identify the clustering region, also used for verification of 700-hPa height; in panel (f) the dashed line identifies the area where observed precipitation data were available for verification. Rms error of 700-hPa height (m) and absolute errors of precipitation (mm/d) are listed above panels (a) –(e), area-averaged precipitation above panel (f).

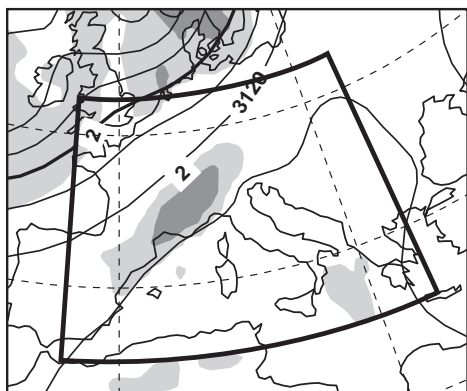
RM 1 - err z700 = 12.76 err TP= 7.64



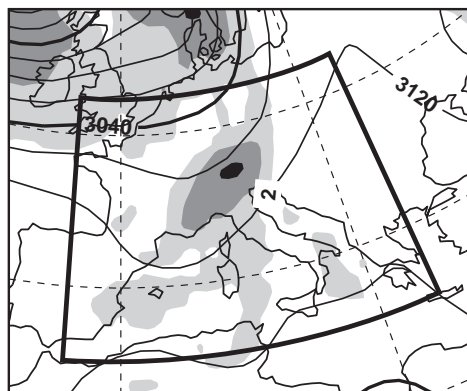
RM 2 - err z700 = 10.61 err TP= 6.25



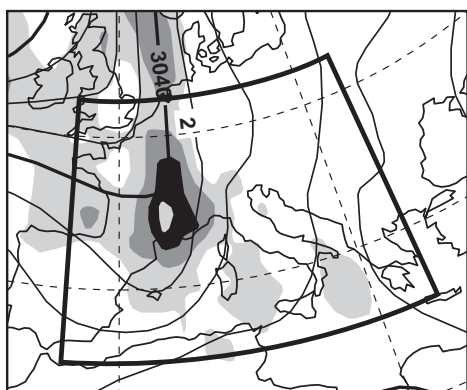
RM 3 - err z700 = 24.59 err TP= 7.46



RM 4 - err z700 = 21.3 err TP= 8.82



RM 5 - err z700 = 23.36 err TP= 8.06



ver - 1992-09-23 12:00:00 - mop=8.76

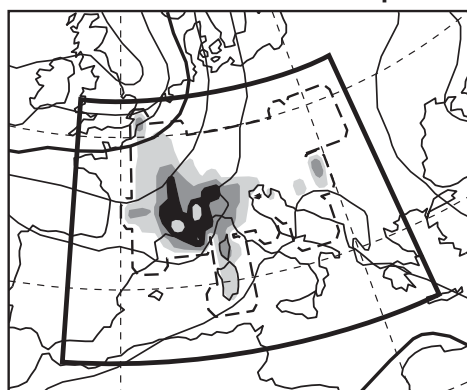


Figure 3 Vaison 1992. As Fig. 2 but for the RMs.

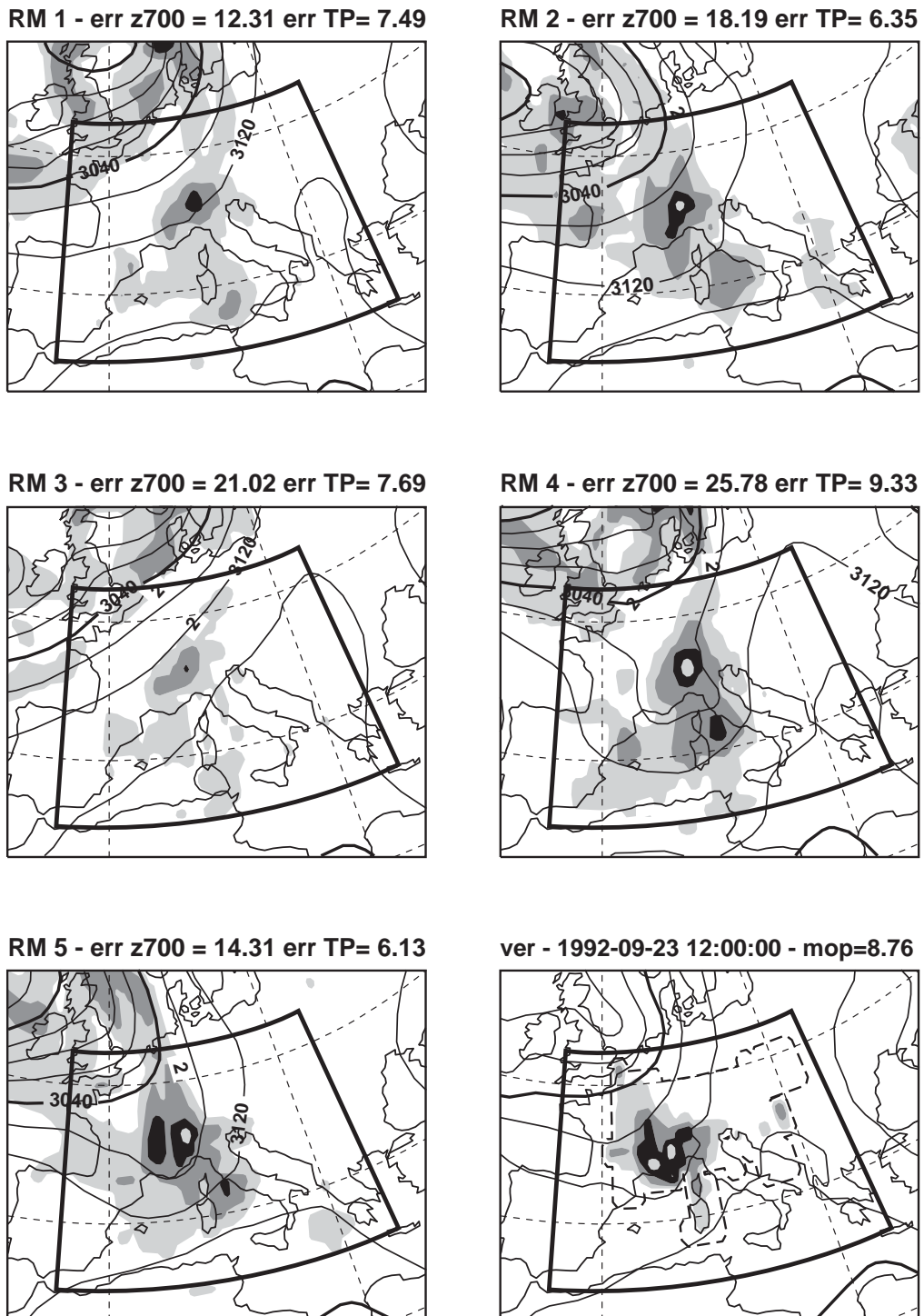


Figure 4 Vaison 1992. As Fig. 2 but for the high-resolution forecasts with initial conditions defined by the low-resolution RMs.

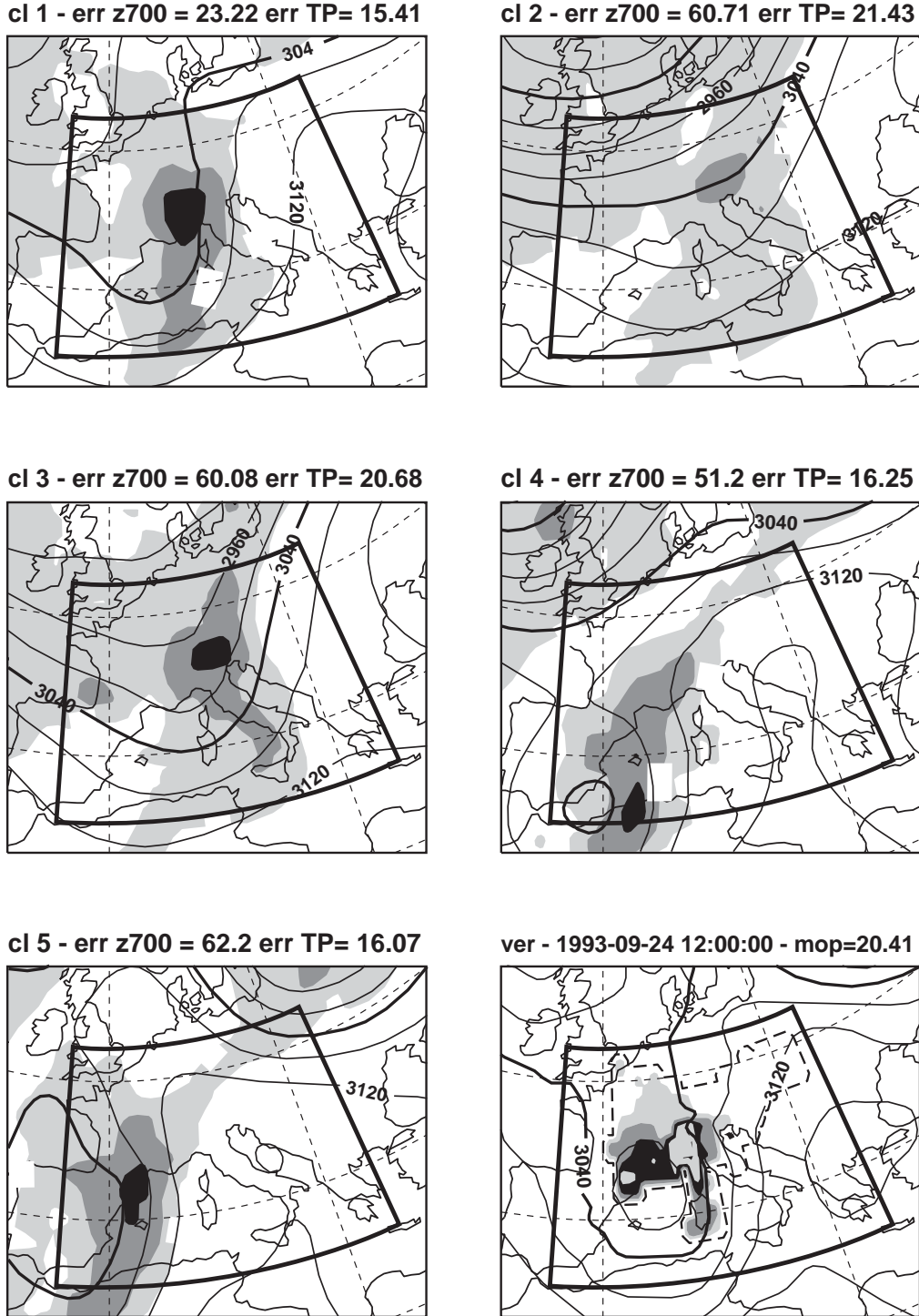
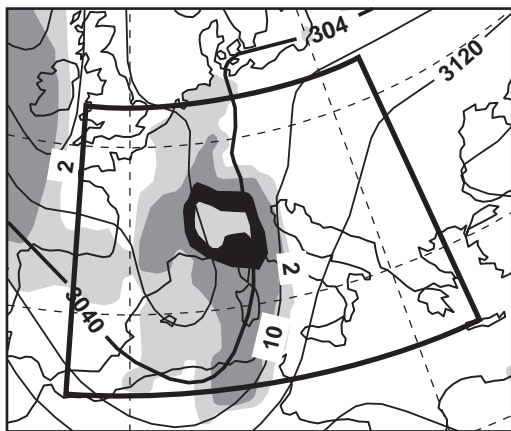
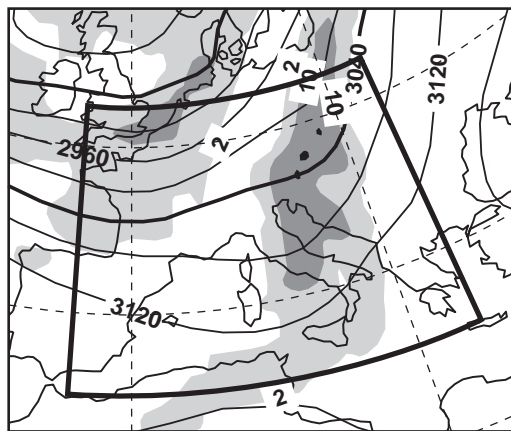


Figure 5 Brig 1993. (a-e) cluster centroids of the 5-day EPS forecasts of 700 hPa geopotential height (valid at 12GMT of 24/9/1993) and of precipitation accumulated in the preceding 24-hours; (f) 700 hPa geopotential height analysis and observed precipitation. Height contour interval 40 m, and precipitation isolines 2, 10, 30 and 60 mm/d.. Rms error of 700 hPa height (m) and absolute errors of precipitation (mm/d) are listed above panels (a)-(e), area-averaged precipitation above panel (f). See Fig. 2 caption for more details.

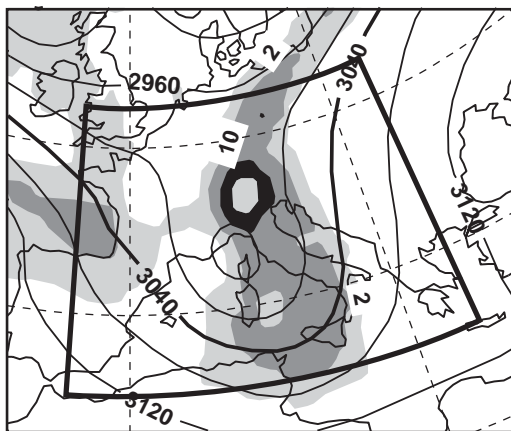
RM 1 - err z700 = 21.47 err TP= 13.93



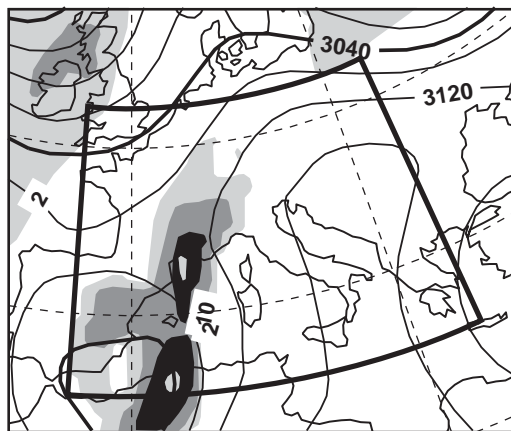
RM 2 - err z700 = 67.94 err TP= 24.86



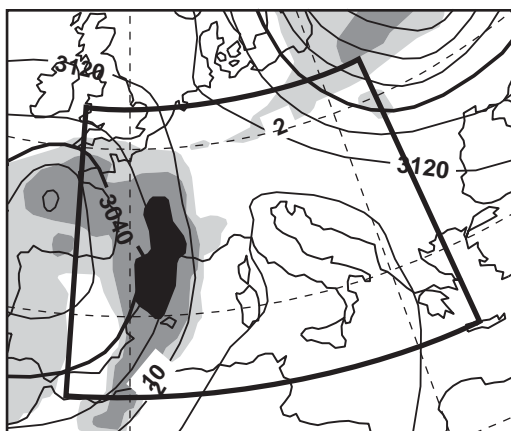
RM 3 - err z700 = 62.25 err TP= 21.99



RM 4 - err z700 = 53.98 err TP= 16.11



RM 5 - err z700 = 72.14 err TP= 17.25



ver - 1993-09-24 12:00:00 - mop=20.41

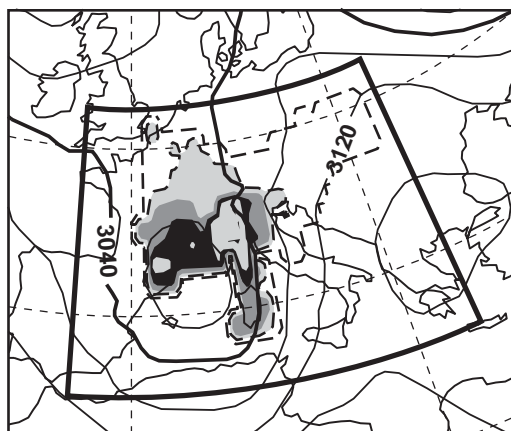


Figure 6. Brig 1993. As Fig. 5 but for the RMs.

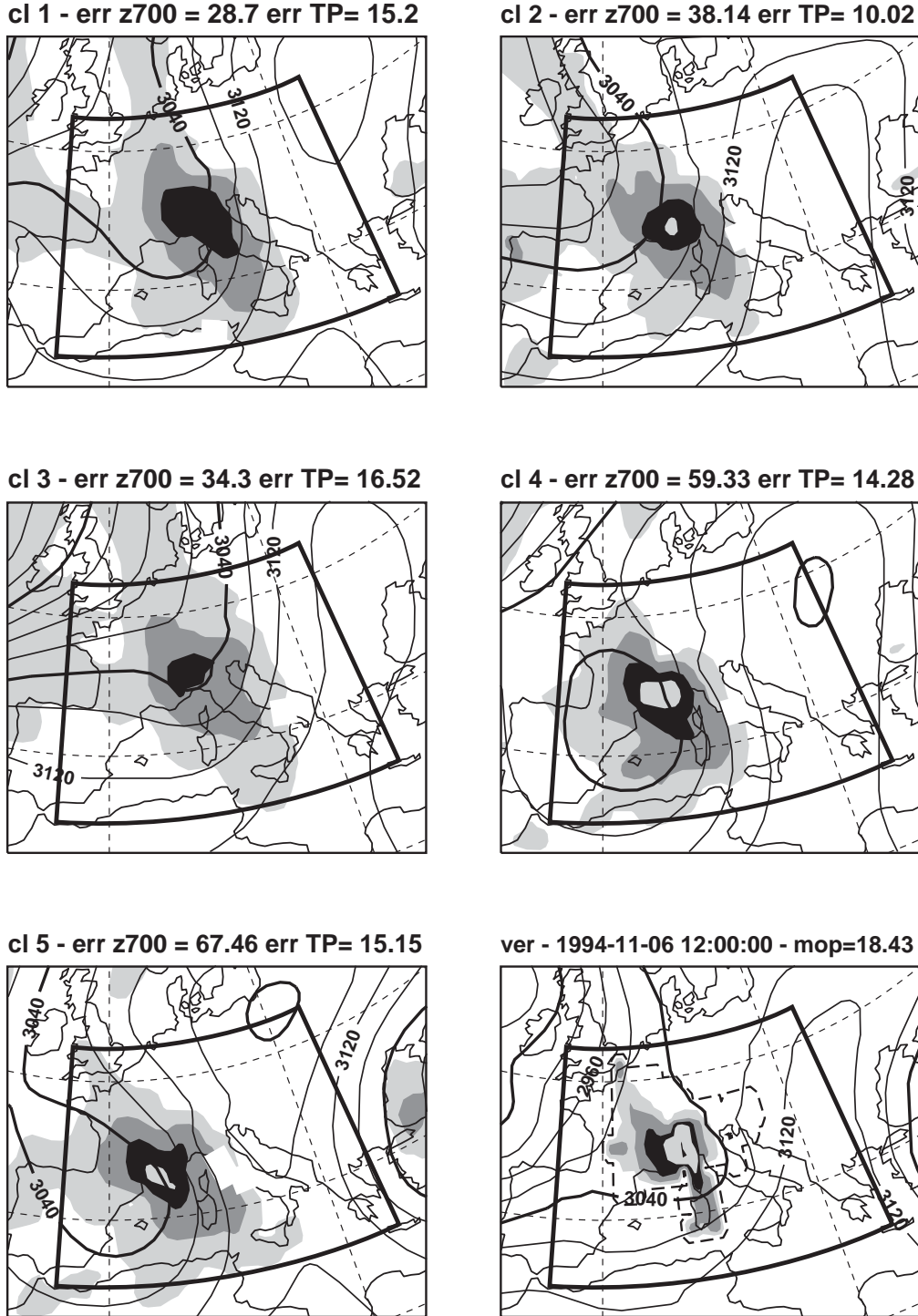
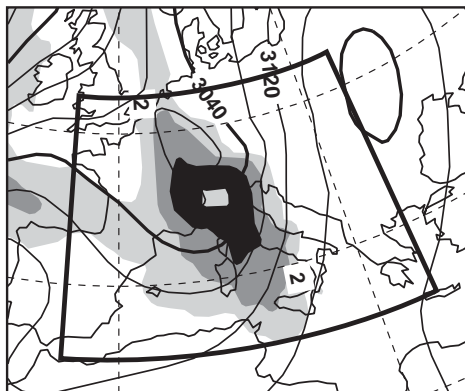
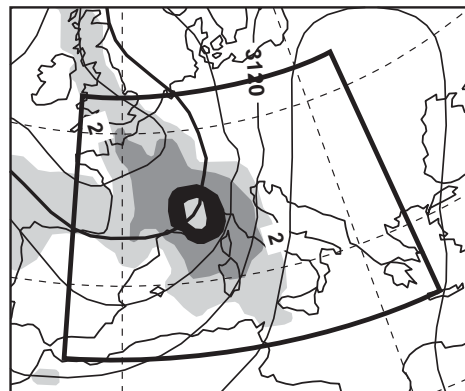


Figure 7. Piemonte 1994. (a-e) cluster centroids of the 5-day EPS forecasts of 700 hPa geopotential height (valid at 12GMT of 6/11/1994) and of precipitation accumulated in the preceding 24-hours; (f) 700 hPa geopotential height analysis and observed precipitation. Height contour interval 40 m, and precipitation isolines 2, 10, 30 and 60 mm/d. Rms error of 700-hPa height (m) and absolute errors of precipitation (mm/d) are listed above panels (a)-(e), area-averaged precipitation above panel (f). See Fig. 2 caption for more details.

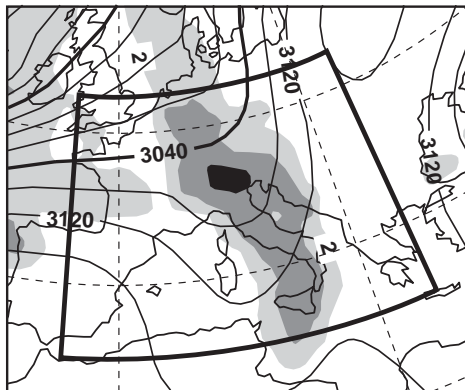
RM 1 - err z700 = 37.4 err TP= 17.72



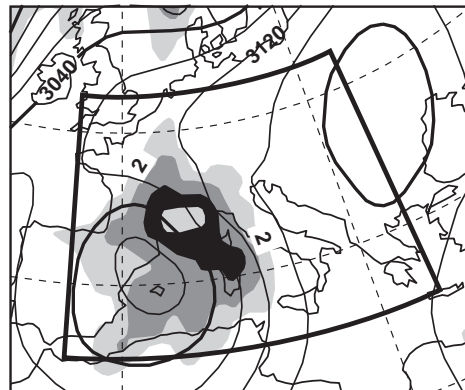
RM 2 - err z700 = 44.86 err TP= 10.26



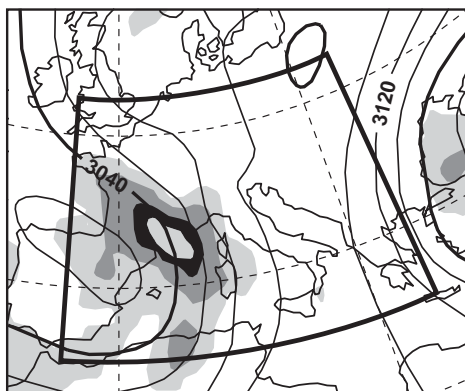
RM 3 - err z700 = 53.13 err TP= 21.88



RM 4 - err z700 = 73.86 err TP= 14.9



RM 5 - err z700 = 74.08 err TP= 19.77



ver - 1994-11-06 12:00:00 - mop=18.43

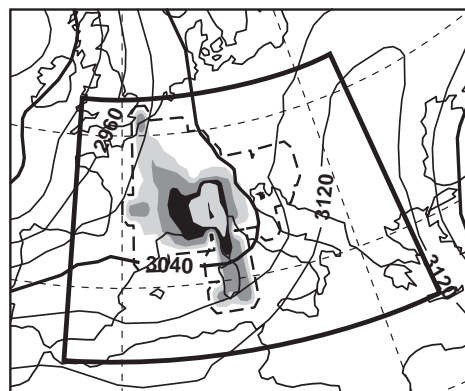


Figure 8. Piemonte 1994. As Fig. 7 but for the RMs.

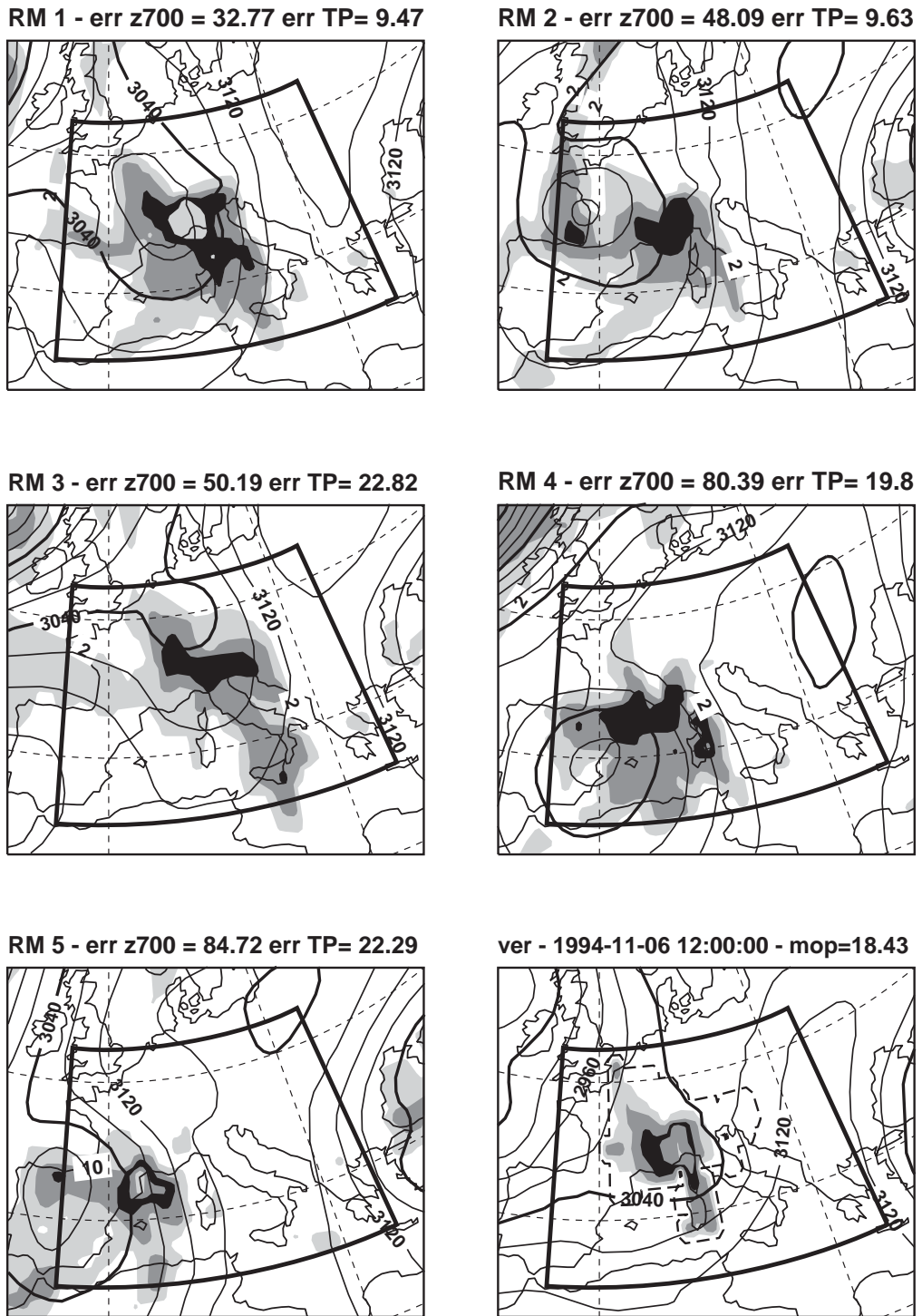


Figure 9. Piemonte 1994. As Fig. 8 but for the high-resolution forecasts with initial conditions defined by the low-resolution RMs.

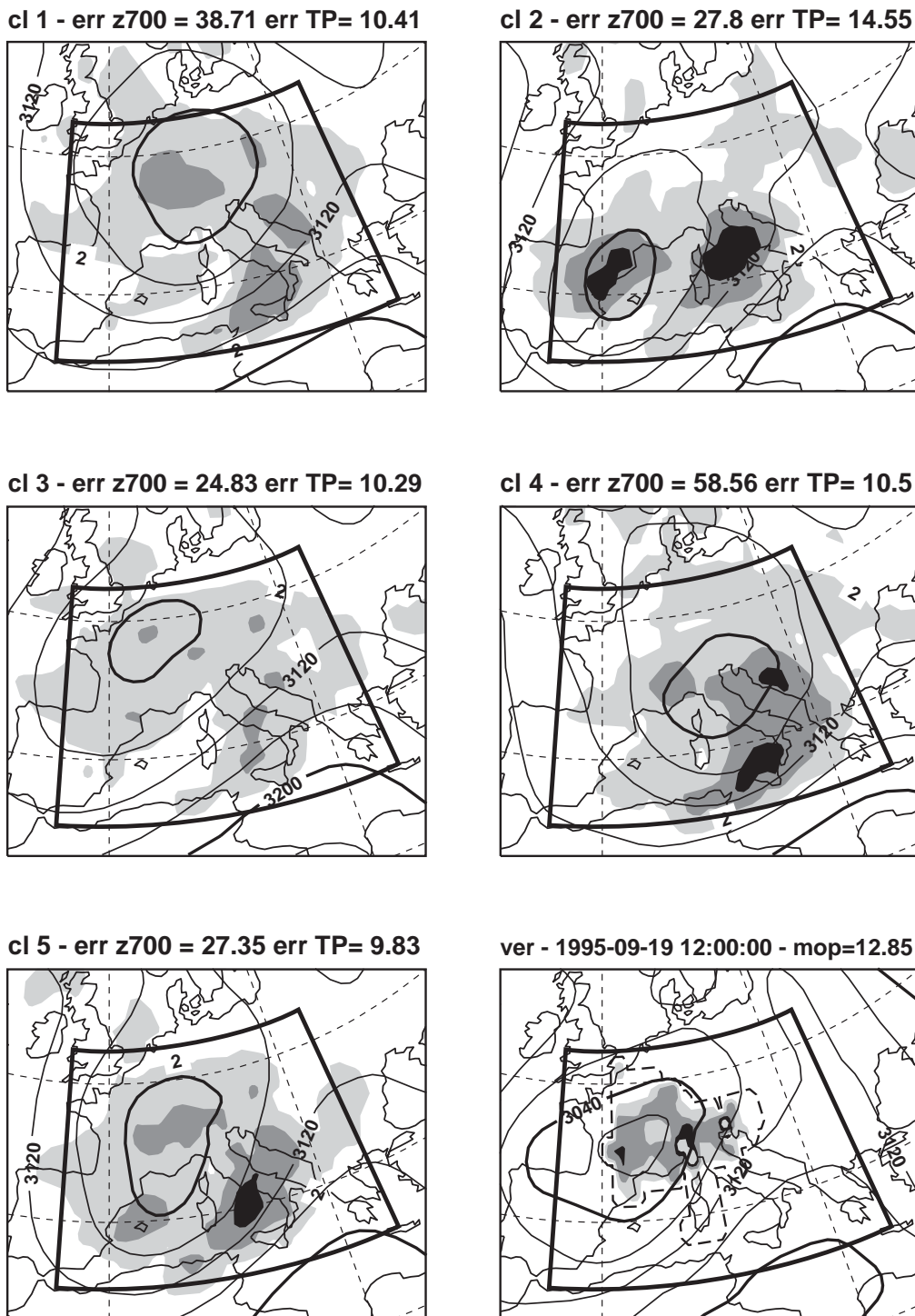


Figure 10. Friuli 1995. (a-e) cluster centroids of the 5-day EPS forecasts of 700 hPa geopotential height (valid at 12GMT of 19/9/1995) and of precipitation accumulated in the preceding 24-hours; (f) 700 hPa geopotential height analysis and observed precipitation. Height contour interval 40 m, and precipitation isolines 2, 10, 30 and 60 mm/d.. Rms error of 700 hPa height (m) and absolute errors of precipitation (mm/d) are listed above panels (a)-(e), area-averaged precipitation above panel (f). See Fig. 2 caption for more details.

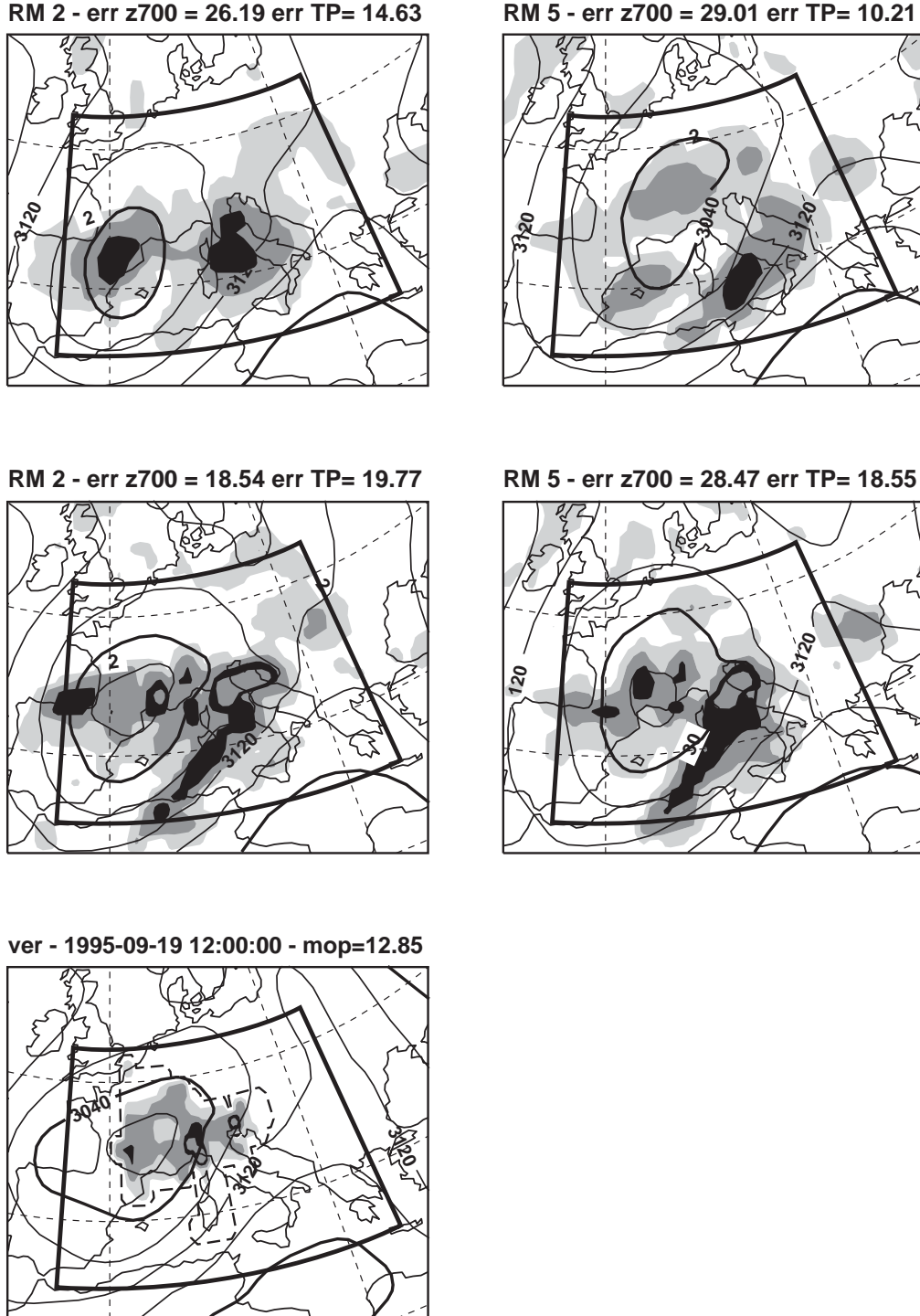


Figure 11. Friuli 1995. (a-b) RMs number 2 and 5 of the 5-day EPS forecasts of 700 hPa geopotential height (valid at 12GMT of 19/9/1995) and of precipitation accumulated in the preceding 24-hours; (c-d) as (a-b) but for the high-resolution resolution forecasts with initial conditions defined by the low-resolution RMs number 2 and 5; (f) 700 hPa geopotential height analysis and observed precipitation. Rms error of 700-hPa height (m) and absolute errors of precipitation (mm/d) are listed above panels (a)–(e), area-averaged precipitation above panel (f). See Fig. 2 caption for more details.

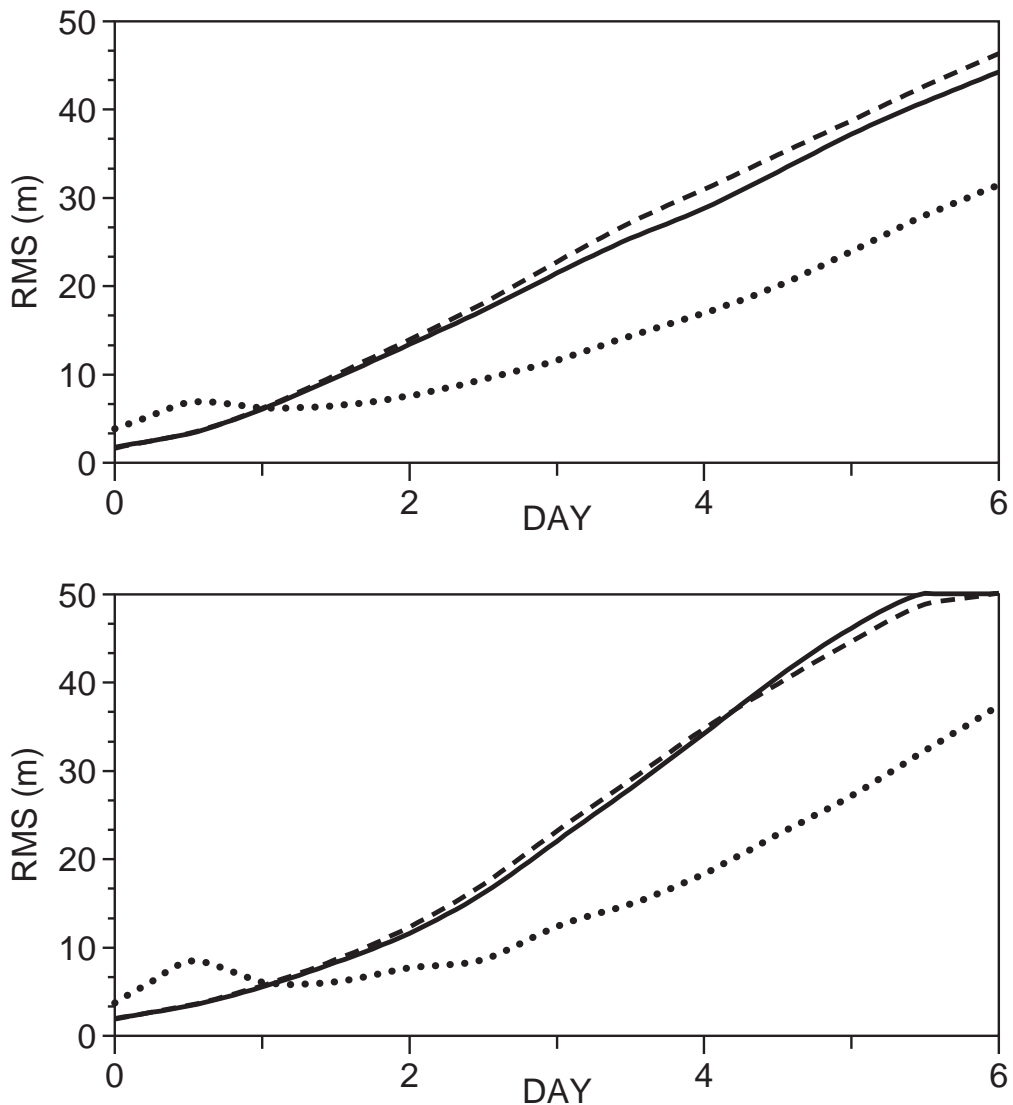


Figure 12. 4-case average of the rms spread of perturbed forecasts from the control for the low- resolution (solid line) and high-resolution (dashed line) ensembles, and of the rms distance between corresponding low- and high-resolution forecasts (dotted line). Values refer to (a) the extra-tropical Northern Hemisphere and (b) to the southern-European region (5°W-25°E; 35°N-53°N).

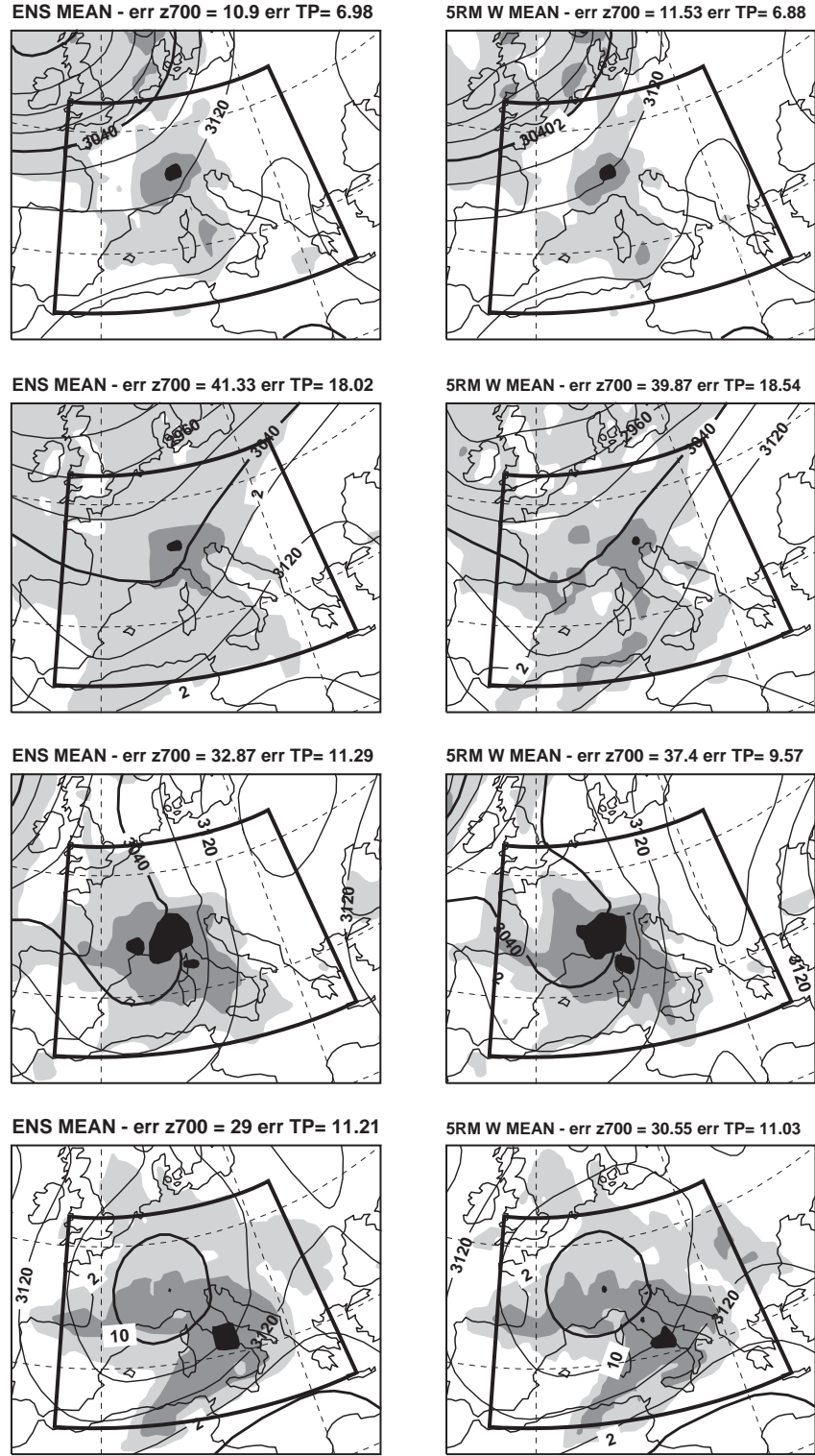


Figure 13. (a-b): ensemble mean forecast at day d+5 from configuration (a) E51H, and (b) E5Hw for Vaison 1992; (c-d): as (a-b) but for Brig 1993; (e-f): as (a-b) but for Piemonte 1994; (g-h): as (a-b) but for Friuli 1995. Height contour interval 40 m, and precipitation isolines 2, 10, 30 and 60 mm/d. The title of each panel lists the rms error for 700 hPa height (m) and the absolute error for precipitation (mm/d).